

# A Simple Model-Free Method for Direct Assessment of Fluorescent Ligand Binding by Linear Spectral Summation

Oktaý K. Gasymov · Adil R. Abduragimov · Ben J. Glasgow

Received: 12 March 2013 / Accepted: 21 August 2013 / Published online: 18 September 2013  
© Springer Science+Business Media New York 2013

**Abstract** Fluorescent tagged ligands are commonly used to determine binding to proteins. However, bound and free ligand concentrations are not directly determined. Instead the response in a fluorescent ligand titration experiment is considered to be proportional to the extent of binding and, therefore, the maximum value of binding is scaled to the total protein concentration. Here, a simple model-free method is presented to be performed in two steps. In the first step, normalized bound and free spectra of the ligand are determined. In the second step, these spectra are used to fit composite spectra as the sum of individual components or linear spectral summation. Using linear spectral summation, free and bound 1-Anilino-naphthalene-8-Sulfonic Acid (ANS) fluorescent ligand concentrations are directly calculated to determine ANS binding to tear lipocalin (TL), an archetypical ligand binding protein. Error analysis shows that the parameters that determine bound and free ligand concentrations were recovered with high certainty. The linear spectral summation method is feasible when

fluorescence intensity is accompanied by a spectral shift upon protein binding. Computer simulations of the experiments of ANS binding to TL indicate that the method is feasible when the fluorescence spectral shift between bound and free forms of the ligand is just 8 nm. Ligands tagged with environmentally sensitive fluorescent dyes, e.g., dansyl chromophore, are particularly suitable for this method.

**Keywords** Fluorescent ligand binding · Tear lipocalin · Direct methods in ligand binding · Polarity sensitive fluorescent ligand · Separative methods · Non-separative methods

## Introduction

Many essential processes in living matter require specific ligand binding and delivery. Molecular recognition between ligands and partner proteins play central role in many biological phenomena. Therefore, characterization of ligand binding to proteins is critical to understand specificity as well as capacity of binding. The accurate quantitative description of ligand binding is fundamental for drug delivery. Numerous methods (spectroscopic, calorimetric, equilibrium dialysis, gel filtration, membrane filtration, etc.) are available to study ligand binding to proteins and to calculate dissociation constants ( $K_d$ ) [1–9]. In most methods, ligands are tagged with various reporter groups, such as spin labels, fluorescent labels, radioisotopes, etc., for selective detection [1, 10–13]. With rare exceptions, e.g., electron paramagnetic resonance (EPR), the majority of spectroscopic techniques do not detect bound and free ligand directly. Therefore, methods have developed to estimate  $K_d$  without knowledge of these components of the ligand [1, 14–16]. The number of publications that use

---

**Electronic supplementary material** The online version of this article (doi:10.1007/s10895-013-1290-y) contains supplementary material, which is available to authorized users.

O. K. Gasymov · A. R. Abduragimov · B. J. Glasgow  
Departments of Ophthalmology, Pathology and Laboratory  
Medicine, Jules Stein Eye Institute, University of California at Los  
Angeles, Los Angeles, CA 90095, USA

O. K. Gasymov (✉)  
100 Stein Plaza, Rm# B267, Los Angeles, CA 90095, USA  
e-mail: ogassymov@mednet.ucla.edu

B. J. Glasgow (✉)  
100 Stein Plaza, Rm# B269, Los Angeles, CA 90095, USA  
e-mail: bglasgow@mednet.ucla.edu

fluorescent binding techniques is rising exponentially (Fig. S1 in the Electronic Supplementary Material). Because intrinsic fluorescence properties of the proteins are not always amenable to ligand binding studies, fluorophore-labeled ligands are used with fluorescence spectroscopy. In the typical titration experiment, the changes in the observable fluorescence parameters, such as intensity, anisotropy value, and  $\lambda_{\max}$ , must be assumed to be proportional to a multiple of the total protein concentration [6, 15, 17].

In this study, bound and free ligand concentrations were determined directly in a fluorescent-ligand titration experiment. Because many fluorescent labels are designed to be environmentally sensitive, fluorescence linear spectral summation is very suitable for a number of such fluorescent ligands. 1-Anilino-naphthalene-8-Sulfonic Acid (ANS), one of the most popular ligands for binding studies with fluorescence spectroscopy, was used as the fluorescent ligand. Tear lipocalin (TL), a promiscuous and archetypical member of the lipocalin family [18, 19] was used as the ligand binding protein. TL is the principal ligand binding protein in tears [19, 20], comprises about 33 % of total proteins in tears, and binds a broad array of endogenous and exogenous ligands [20–24]. Binding of fluorescent ligands to TL, including ANS, has been extensively studied [21, 25–27]. The studies were done using the traditional indirect method. The strategy presented here, linear spectral summation, yields bound and free ligand concentrations and is widely applicable for fluorescent-ligand complexes of many proteins.

## Material and Methods

### Materials

1-Anilino-naphthalene-8-Sulfonic Acid (ANS, high purity) was purchased from Invitrogen (San Diego, CA). Other chemicals used to prepare various buffers were purchased from Sigma-Aldrich (St. Louis, MO).

### Mutagenesis and Plasmid Construction

The cDNA of TL in PCR II (Invitrogen) [28], was used as a template to clone the TL gene spanning bases 115–592 of the previously published sequence [19] into pET 20b (Novagen, Madison, WI). Flanking restriction sites for NdeI and BamHI were added to produce the native protein sequence but with the addition of an initiating methionine [29]. For ANS binding the W17Y/F130W (W130 for simplicity) mutant of TL, was used as a part of an ongoing research project. W130 was constructed with oligonucleotides (Universal DNA) using the previously published method of introduction of a point mutation by sequential PCR steps as previously described [21].

### Expression and Purification of Proteins

The mutant plasmid was transformed in *E. coli*, BL 21 (DE3), cells were cultured, and protein was expressed as indicated by the manufacturer's protocol (Novagene). Cell lysis and protein purification were performed as described previously [30]. Purity of the proteins was verified by SDS tricine gel electrophoresis [20]. The protein concentration for W130 was determined using a molar extinction coefficient  $\epsilon_{280} = 15,040 \text{ M}^{-1} \text{ cm}^{-1}$  calculated on the basis of the tyrosine added to TL,  $\epsilon_{280} = 13,760 \text{ M}^{-1} \text{ cm}^{-1}$  [31].

### Absorption Spectroscopy

UV absorption spectra were measured using Shimadzu UV-2400PC spectrophotometer. To determine the protein concentration more precisely, a minor contribution of the light scattering to the absorption spectra was corrected by plotting the log of absorbance of the solution versus the log of the wavelength and extrapolating the linear dependence between these quantities in the range 330–390 nm to the absorption range 240–330 nm.

### CD Measurements

To confirm that the mutant has a native fold, far-UV CD spectra were recorded (Jasco 810 spectropolarimeter, 0.2 mm path length) using a protein concentration of 1.2 mg/ml. Eight scans from 190 to 260 nm were averaged. The CD spectrum of W130 is similar in  $\alpha$ -helical and  $\beta$ -sheet content to the wild type protein indicative of the native lipocalin fold (data not shown and will be published elsewhere).

### Steady-state Fluorescence Spectroscopy

Steady-state fluorescence measurements were made on a Jobin Yvon-SPEX (Edison, NJ) Fluorolog tau-3 spectrofluorometer, bandwidth for excitation and emission were 2 nm and 3 nm, respectively. The excitation  $\lambda$  was 335 nm. The concentration of methanol stock solution of ANS was confirmed by absorbance at 372 nm, using an extinction coefficient,  $\epsilon_{335} = 7,800 \text{ M}^{-1} \text{ cm}^{-1}$  (Invitrogen). The fluorescence spectra were corrected for light scattering from buffer.

### Fluorescence Binding Assays by Spectral Summation (Direct or Separative Method)

The TL mutant, W130 (2.8  $\mu\text{M}$ ) in 10 mM sodium phosphate at pH 7.3 was titrated by addition of ANS and the fluorescence spectra were measured. Following each addition of ANS, the solution was mixed and allowed to equilibrate for 2 min. At the end of the titration experiment, the methanol concentration

did not exceed 2 %. For this method two scaled spectral measurements, bound and free ANS spectra, are enough to fully characterize the binding experiment. To obtain the bound ANS spectrum, mixture of 0.3 μM ANS and 20 μM W130 in 10 mM sodium phosphate at pH 7.3 were prepared and fluorescence spectrum was measured. The molar excess of TL ensures that all ANS molecules are bound to the protein. The free ANS spectrum was obtained using 16.9 μM ANS solution (without any protein) in the buffer. Each composite spectrum from the titration experiment was recomposed by fitting scaled bound (0.3 μM) and free (16.9 μM) ANS spectra using a program created in LabView (National Instruments, Austin, TX). In addition, a baseline component was added for better quality fit. The program uses the “General linear Fit VI” subVI to fit each experimental spectrum to the linear summation of the components. The number of components that can be added is not limited; however, in this study two components (excluding the baseline) were satisfactory to fit all titration spectra. The calculated composite spectrum ( $S_{cal}$ ) is

$$S_{cal} = (k_{bound}c_{bound}S_{bound}) + (k_{free}c_{free}S_{free})$$

where,  $S_{bound}$  and  $S_{free}$  are the standard bound and free ANS spectra, respectively. The  $k_{bound}$  and  $k_{free}$  are scaling parameters for the bound and free ligands, respectively. The  $c_{bound}$  and  $c_{free}$  are input parameters (in this study, 0.3 μM and 16.9 μM, respectively) for the concentrations of the standard bound and free ligands, respectively. Thus, unknown molar concentrations of the ligands are determined as  $L_{bound} = k_{bound}c_{bound}$  and  $L_{free} = k_{free}c_{free}$ . The best fit is accomplished by scaling the coefficients of each component. The quality of fit is judged by  $\delta_n$  (normalized-root-mean-square-deviation) that was calculated by the following formula:

$$\delta_n = \sqrt{\frac{\sum_n (I_i^{exp} - I_i^{cal})^2}{\sum_n (I_i^{cal})^2}}$$

where  $I_i^{exp}$  and  $I_i^{cal}$  are the sequence of the experimental and calculated spectral data, respectively.

In this method, all spectra can be normalized to the same amplitude. Normalization of the sum of the coefficients  $L_{bound} + L_{free} = L_{total}$ , i.e., total concentration of ANS, to the experimental values yields identical results with that of the unnormalized experimental spectra. It means that if one has standard spectra for a given protein, characterization of ligand binding via this method does not depend on sensitivity of the device. In fact, a binding experiment can be performed on various devices, but similar settings should be used to be sure that spectral width and position are not changed. The ligand binding data derived from spectral summation were analyzed by non-linear curve fitting to the following formula using

OriginPro 8 software (OriginLab Corp., Northampton, MA):

$$L_{bound} = \frac{B_{max}L_{free}}{K_d + L_{free}} \tag{1}$$

where,  $L_{bound}$  and  $L_{free}$  are the bound and free ANS concentrations, respectively,  $K_d$  is the dissociation constant,  $B_{max}$  is maximum bound concentration and stoichiometry ( $n$ ) was determined as  $B_{max}/P_{total}$ , where  $P_{total}$  is total protein concentration. In addition, for convenience of some readers, Scatchard analysis of the same data was performed. For a reader who is not familiar with LabView programming, it should be noted that summation of the spectral components to fit the observed spectra (the formula above shown for  $S_{cal}$ ) could be performed by fitting with multiple independent variables using Origin software.

The uncertainty of the determined parameters was accessed via the  $F$ -statistics, ratio of  $\chi^2/\chi^2_{min}$  was determined.  $\chi^2$  was determined as:

$$\chi^2 = \sum_i (f_i - y_i)^2$$

$f_i$  and  $y_i$  are the sequence of fitted and experimental values, respectively. Details of the statistics were previously described elsewhere [32, 33]. Briefly, fitting was performed to determine the parameters that correspond to the minimum  $\chi^2_{min}$  value. Then one parameter was fixed to various values while allowing variation in the values of the other component to minimize  $\chi^2$  to a new value.  $F_\chi$  was estimated to be 1.08 for the probability value of 0.32.

### Computer Simulations of ANS Binding to TL with Various Fluorescence Spectral Shifts

In TL, the difference between the fluorescence  $\lambda_{max}$  values of ANS in bound and free forms is about 55 nm. To assess the limit of applicability of the current method we have simulated a series of composite spectra in which ratio of bound/free was identical to that of found in the experimental data. However, in each series, position of the experimental free ANS spectrum ( $\lambda_{max}$  520 nm) was blue-shifted (39 nm, 44 nm and 49 nm, respectively). To make it similar to the experimental data, 3 % random noise was added to each simulated spectrum. The linear spectral summation method was applied to each set of simulated experiment and the validity of the model was judged by adjusted  $R^2$  data of the linear regression analysis.

## Fluorescence Binding Assays by the Indirect (Non-separative) Method

For comparison, we analyzed the same experimental data for ANS and TL (W130) by a more traditional method [6, 15, 16, 24]. In this assay, fluorescence intensities at 460 nm were used. The ligand binding data were analyzed with the following formula for one binding site using OriginPro 8 software:

$$y = 0.5F \left[ (P_t + K_d + L_t) - \sqrt{(P_t + K_d + L_t)^2 - 4L_tP_t} \right] \quad (2)$$

where  $F$  is a fluorescence scaling factor,  $K_d$  is the apparent dissociation constant,  $P_t$  is total protein concentration,  $L_t$  is the total ligand concentration, and the stoichiometry is assumed to be 1. A titration curve was corrected for the free ANS contribution. The correction is not a trivial procedure, because for each data point, the concentration of free ANS should be estimated for subtraction using the calibration curve [15]. This procedure is also done with the assumption that the ligand binding to the protein is 1:1. Another disadvantage of this method is that the contribution of the fluorescence of the free ligand and therefore the  $K_d$  value depends on the wavelength chosen for analysis. If in this case 466 nm  $\lambda_{\max}$  were chosen for analysis, the contribution to fluorescence of the free ligand would be greater than if 460 nm were chosen. Without knowledge of the stoichiometry the resulting error in the  $K_d$  value could not be accurately corrected.

## Results and Discussion

ANS binding to native TL as well as to many of its numerous mutants has been studied previously [23, 25, 34]. ANS binds within the cavity of TL [23] that results in an enhancement of the fluorescence intensity and a blue shift in fluorescence  $\lambda_{\max}$  (Fig. 1). ANS displays minimal fluorescence in an aqueous environment with a fluorescence  $\lambda_{\max}$  of about 520 nm. Upon binding to W130, ANS fluorescence  $\lambda_{\max}$  blue shifts to 466 nm and fluorescence intensity increases about 30 fold (Fig. 1a). Figure S2 in the Electronic Supplementary Material (ESM) shows the fluorescence spectra at various concentrations of ANS with a constant concentration of W130 (2.8  $\mu\text{M}$ ). As an example, the recombination from summed bound and free components (along with determined concentrations) are also shown in Fig. 1 (recomposition of the fluorescence spectra for all ligand concentrations are provided in Fig. S2 in the ESM). All spectra are well fit to a sum of the two components. The free ANS fluorescence spectrum does not contribute much to the blue side (<450 nm) of the spectra, whereas the bound ANS spectrum contributes significantly (Fig. 1). Despite the fact that free ANS fluorescence has very

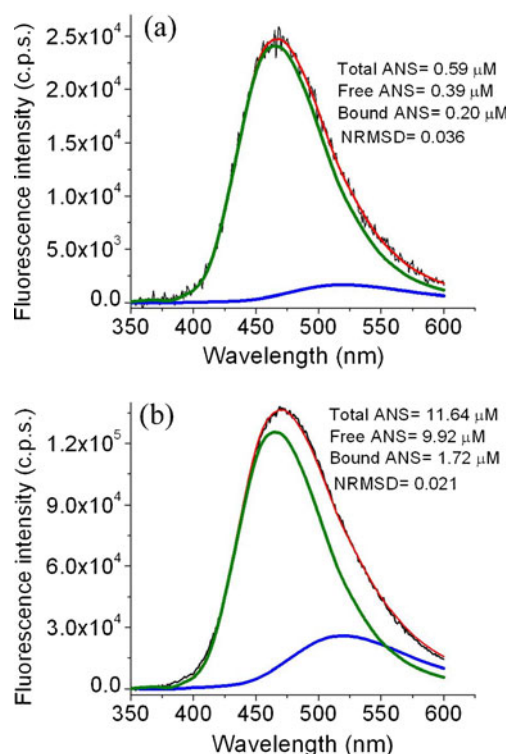


**Fig. 1** Decompositions of ANS fluorescence spectra of ANS-TL complexes into bound and free components in the ligand titration experiment. Concentration of the protein was constant, 2.8  $\mu\text{M}$ . Total ANS concentrations: **a** 0.59  $\mu\text{M}$ ; **b** 11.64  $\mu\text{M}$ . Black, red, olive and blue lines represent experimental, best fit to two component spectra, fraction of bound and free ANS spectra, respectively. Decompositions of the ANS fluorescence spectra for all ligand concentrations are provided in Fig. S2 in the ESM

little intensity, their contributions in the region of >520 nm exceed that of bound ANS at concentrations >8  $\mu\text{M}$  (total ANS) (Fig. S2 in the ESM). The  $\delta_n$  values are below 0.036 for all of the best fits and experimental spectra. Inspection of the residuals is also indicative of good fits (Fig. S3 ESM).

Low  $\delta_n$  values are necessary but not enough to determine the parameters explicitly. The uncertainty of the determined parameters is reflected in a support plane analysis (Fig. 2). Examination of the  $\chi_R^2$  surfaces provides valuable information about the resolution of the scaling parameters. As an example W130 (2.8  $\mu\text{M}$ )-ANS (11.64  $\mu\text{M}$ ) is shown. Steep  $\chi_R^2$  surfaces were found for both parameters (Fig. 2); the parameters were recovered with high certainty.

Area normalized fluorescence spectra of ANS-W130 complexes are shown in Fig. 3. The data suggest two important points for ligand binding analysis. Firstly, a sharp isosbestic point observed at about 495 nm verifies that the fluorescence spectra are composed of two species (bound and free). Secondly, the integral fluorescence intensities (areas under the fluorescence curves) are proportional to corresponding (bound or free) ligand concentrations, otherwise an isosbestic point could not be observed.



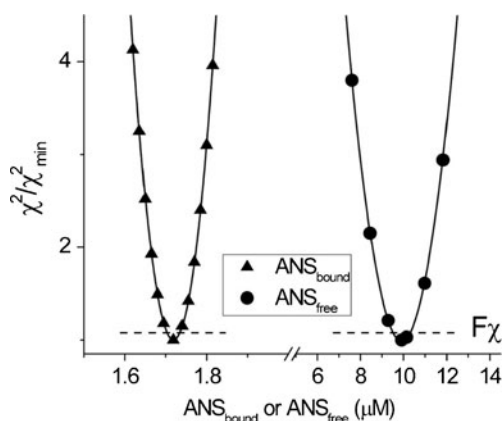


**Fig. 2** Error analysis for the best fit performed for the ANS (11.64 μM)-W130 (2.8 μM) complex. The bound and free concentrations of ANS are estimated to be 1.72 μM and 9.92 μM, respectively

By summation from just two standard spectra, pure free and bound components, with subsequent fitting the individual concentrations of bound and free ligands in any composite spectra are revealed. The method does not require any additional assumptions, such as scaling intensity to protein concentration and stoichiometric relationships. The data recovered from the results shown in Fig. S2 ESM are plotted in Fig. 4. Both plots, rectangular hyperbola (Fig. 4a, formula (1)) and Scatchard (Fig. 4b), indicate good fits and almost identical results ( $K_d = 4.3 \pm 0.2 \mu\text{M}$ ). Stoichiometry of ANS binding to W130 is close to 1:1 ( $n = 0.87 \pm 0.05$ ). It should be emphasized that the stoichiometry value is the derived datum and is not the result of an assumption of 1:1 binding. In the traditional method curve fitting is performed under an assumed stoichiometric relationship. To appreciate the spectral summation method, the data were also analyzed by using the fluorescence intensity at 460 nm (Fig. 5) and fitting to the formula (2). Data were corrected for the free ANS contribution as described above. Compared to the spectral summation method, the estimated  $K_d$  value is more than 2 fold lower,  $1.8 \pm 0.2 \mu\text{M}$ . For some studies, the differences in  $K_d$  values determined by these two methods

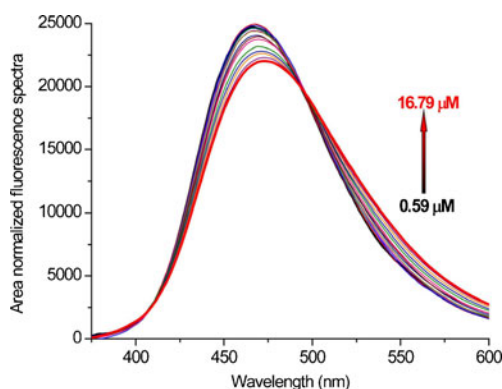


**Fig. 3** Area normalized fluorescence spectra of various concentrations of ANS with W130 (constant, 2.8 μM). An isosbestic point is apparent at about 495 nm. Noise reduction of the spectra was performed for clarity. The procedure did not induce any changes in the shapes of the spectra

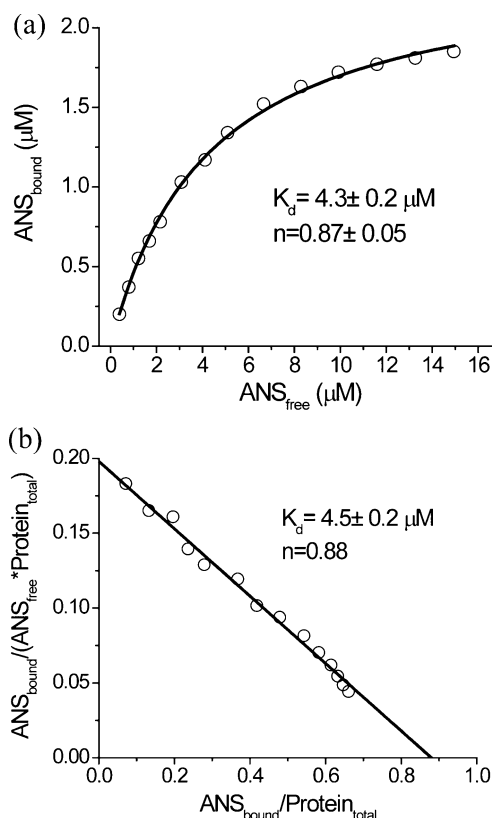


**Fig. 4** ANS binding to TL (W130) derived from linear spectral summation method (Fig. S2). Solid lines are the best fits for a rectangular hyperbola (formula 1) in (a) and linear regression for Scatchard plot in (b)

may be considered insignificant. However, actual stoichiometry data are lacking for the indirect method and must be assumed. Therefore, the spectral summation method will be very valuable in binding studies with varied stoichiometry.

In TL, upon binding the fluorescence  $\lambda_{\text{max}}$  of the free ANS (520 nm) shifts the blue side of the spectrum, about 54 nm (466 nm). The spectral shifts observed for environmental sensitive chromophores depend on hydrophobicity of the

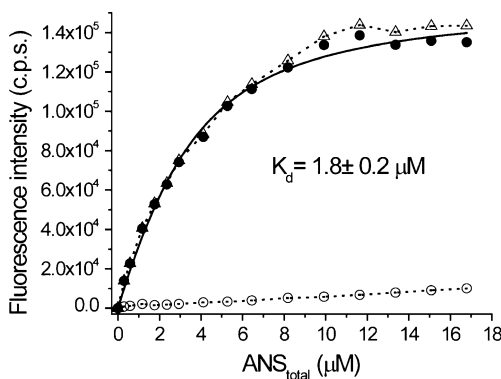


**Fig. 5** Fluorescence intensity ( $\lambda = 460 \text{ nm}$ ) as a function of varying concentrations of ANS with the protein, W130 (2.8 μM). Solid circles- experimental data corrected for the contribution of free ANS; open triangles- experimental data, open circles- free ANS intensity, solid line- best fit to the one binding site (formula 2)

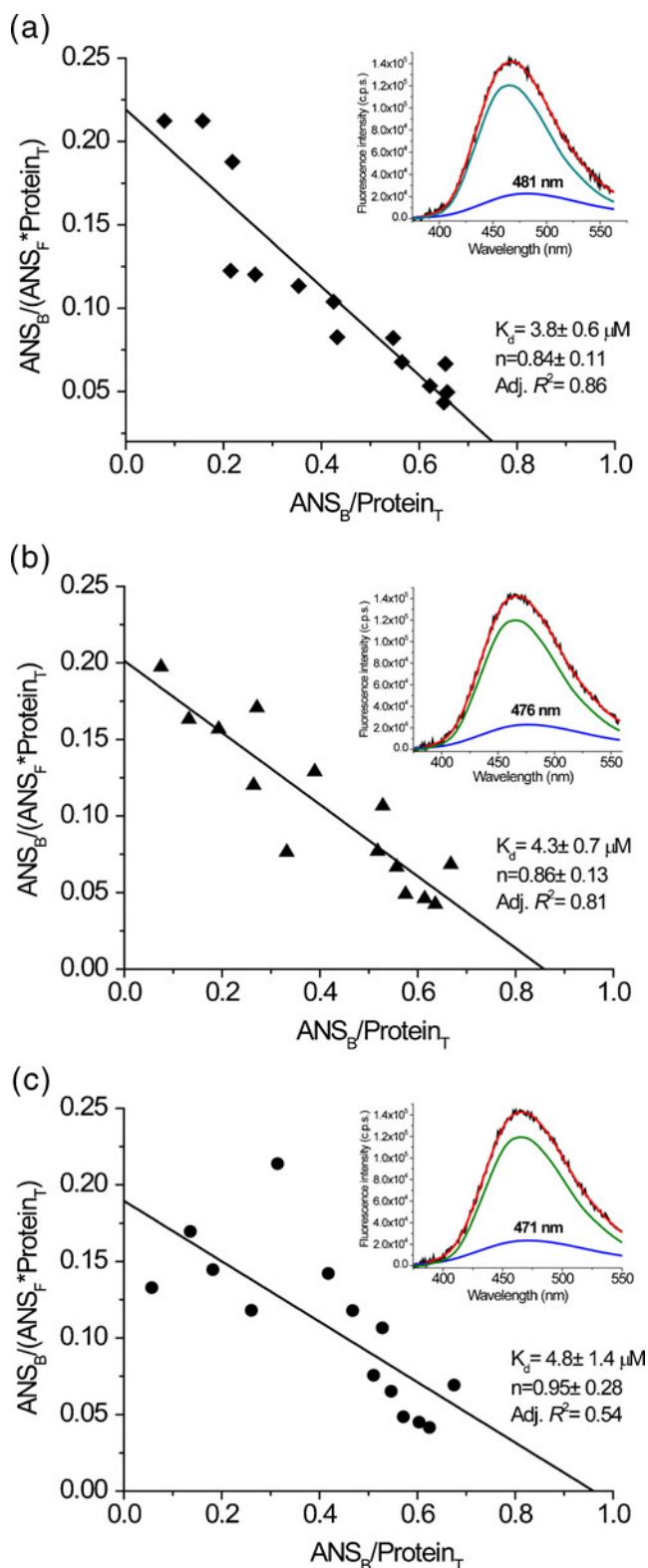


**Fig. 6** Computer simulation of ANS binding to TL with various spectral shifts. **a–c** linear regressions for Scatchard plots for spectral shifts of 39 nm, 44 nm, 49 nm, respectively. Data points were recovered from linear spectral summation method shown in Fig. S4–S6, respectively; Insets: black, red, olive and blue lines represent simulated (total ANS=9.9  $\mu\text{M}$ ), best fit to two component spectra, fraction of bound and free ANS spectra, respectively. The positions of the fluorescence  $\lambda_{\text{max}}$  of simulated free ANS spectra are shown

binding sites. Therefore, upon binding the same chromophore will display various spectral shifts for different proteins. To determine the limit of applicability of the method, a series of composite spectra with different spectral shifts values were simulated (see “Material and Methods” for details) and subjected to the same analysis (Fig. 6). The spectral fitting data for these series are shown in Fig. S4–S6 ESM. Upon decrease of the spectral shifts, binding data appear more scattered in Scatchard plots. As consequences, adjusted  $R^2$  values decrease indicating a worse goodness of the fit (Fig. 6). The recovered data for binding are similar to that of the experimental data. The dependence of the  $R^2$  values on the spectral shift reveals that about 8 nm shift of ANS spectrum is enough for analysis of the binding data by the linear spectral summation method (Fig. 7).

The method is applicable to a variety of polarity sensitive ligands, such as dansyl labeled fatty acid and phospholipids; anilino-naphthalenesulfonate (ANS) and related derivatives; naphthalene derivatives (acrylodan, prodan, laurdan); dapoxyl derivatives [35–39]. The method should be also very effective in competitive ligand binding assays, in which native ligands displace the bound fluorescent ligand [40, 41].

A direct assessment of the bound and free spin labeled ligands can also be performed with EPR [13, 21]. However, EPR requires complex equipment, special expertise, and a limited selection of spin labeled ligands are available. The experiments require higher concentrations of ligand and protein that often approach the limits of solubility. These shortcomings may make EPR impractical for many laboratories. Linear spectral summation can be applied to UV spectroscopy and would be highly accessible to biochemistry laboratories. However, the shifts accompanying ligand binding are often small compared to fluorescence. The advantages of spectral summation in fluorescence spectroscopy are the accessibility of steady state fluorometers, the wide repertoire of available fluorescent ligands and the sizeable spectra shift that often accompanies ligand binding.

A litany of various multivariate linear-response spectroscopic techniques have been developed and applied to many

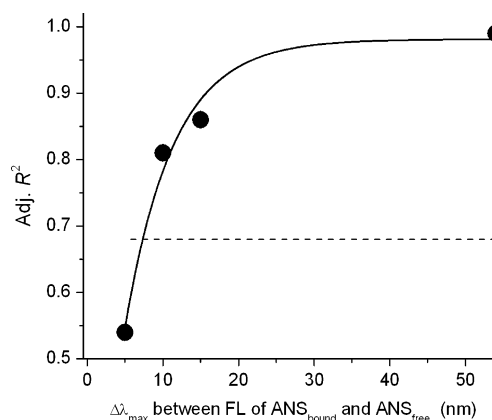


**Fig. 7** The dependence of the  $R^2$  values on the spectral shift of free ANS spectrum. Dashed line indicates the  $R^2$  value of 0.68

ligand-binding events [42, 43]. In cases where spectral characteristics of individual species are unknown, various binding models are required, which impose additional constraints to solve the problem. Use of various binding models to decompose matrix (dose dependent multivariate spectroscopic data) is also referred as a “hard-modeling” method. In contrast, a “soft-modeling” method does not use an explicit model in calculations and is designed to recover a binding model from data analysis. The method requires the estimation of matrixes with local rank and pure variable detection methods. Applications and limitations of both methods were reviewed [44]. In contrast, our proposed method is simple, model free and does not require complex software. One experimentally acquires spectral components of individual species, bound and free spectra of ligand. In addition, applicability of two species in binding as well as linearity of their response can be tested. Concentration normalized spectra will not display an isosbestic point if one of the above-mentioned conditions fails. The method is easy to apply for many ligand-binding events in which researchers use just fluorescence intensity at one wavelength. The experimentally determined stoichiometry value ( $n$ ) may be used as quality control in mutant productions of many ligand-binding proteins. Values of  $n$  less than 1 may indicate higher oligomer formation and/or the presence of misfolded proteins, without ligand binding. However, this information will be overlooked if one uses the “indirect method” described above. Therefore, the direct method using linear spectral summation will be widely applicable for routine binding assay applications.

**Acknowledgments** This work was supported by U.S. Public Health Service grants NIH EY11224 and EY00331 as well as the Edith and Lew Wasserman Endowed Professorship in Ophthalmology (BG).

## References

- Vuignier K, Schappler J, Veuthey JL, Carrupt PA, Martel S (2010) Drug-protein binding: a critical review of analytical tools. *Anal Bioanal Chem* 398 (1):53–66. doi:10.1007/s00216-010-3737-1
- Kariv I, Cao H, Oldenburg KR (2001) Development of a high throughput equilibrium dialysis method. *J Pharm Sci* 90(5):580–587. doi:10.1002/1520-6017(200105)90:5<580::AID-JPS1014>3.0.CO;2-4
- Oravcova J, Bohs B, Lindner W (1996) Drug-protein binding sites. New trends in analytical and experimental methodology. *J Chromatogr B Biomed Appl* 677(1):1–28
- Kansy M, Senner F, Gubernator K (1998) Physicochemical high throughput screening: parallel artificial membrane permeation assay in the description of passive absorption processes. *J Med Chem* 41(7):1007–1010. doi:10.1021/jm970530e
- Hage DS, Tweed SA (1997) Recent advances in chromatographic and electrophoretic methods for the study of drug-protein interactions. *J Chromatogr B: Biomed Sci Appl* 699(1–2):499–525
- Jameson DM, Mocz G (2005) Fluorescence polarization/anisotropy approaches to study protein-ligand interactions: effects of errors and uncertainties. *Methods Mol Biol* 305:301–322. doi:10.1385/1-59259-912-5:301
- Johnson ML (1985) The analysis of ligand-binding data with experimental uncertainties in the independent variables. *Anal Biochem* 148(2):471–478
- Johnson ML, Straume M (2000) Deriving complex ligand-binding formulas. *Methods Enzymol* 323:155–167
- VanScyoc WS, Sorensen BR, Rusinova E, Laws WR, Ross JB, Shea MA (2002) Calcium binding to calmodulin mutants monitored by domain-specific intrinsic phenylalanine and tyrosine fluorescence. *Biophys J* 83(5):2767–2780. doi:10.1016/S0006-3495(02)75286-7
- Lobel D, Marchese S, Krieger J, Pelosi P, Breer H (1998) Subtypes of odorant-binding proteins—heterologous expression and ligand binding. *Eur J Biochem* 254(2):318–324
- Darwish Marie A, Veggerby C, Robertson DH, Gaskell SJ, Hubbard SJ, Martinsen L, Hurst JL, Beynon RJ (2001) Effect of polymorphisms on ligand binding by mouse major urinary proteins. *Protein Sci* 10(2):411–417. doi:10.1110/ps.31701
- Ahnstrom J, Faber K, Axler O, Dahlback B (2007) Hydrophobic ligand binding properties of the human lipocalin apolipoprotein M. *J Lipid Res* 48(8):1754–1762. doi:10.1194/jlr.M700103-JLR200
- Narayan M, Berliner LJ (1997) Fatty acids and retinoids bind independently and simultaneously to beta-lactoglobulin. *Biochemistry* 36(7):1906–1911
- Le Bonniec B, Sauloy J, Ducrocq R, Elion J (1988) Analysis of ligand-binding data without knowledge of bound or free ligand molar concentration. *Anal Biochem* 174(1):280–290
- Cogan U, Kopelman M, Mokady S, Shinitzky M (1976) Binding affinities of retinol and related compounds to retinol binding proteins. *Eur J Biochem* 65(1):71–78
- Ribeiro MM, Franquelim HG, Castanho MA, Veiga AS (2008) Molecular interaction studies of peptides using steady-state fluorescence intensity. Static (de)quenching revisited. *J Pept Sci* 14(4):401–406. doi:10.1002/psc.939
- Otagiri M, Masuda K, Imai T, Imamura Y, Yamasaki M (1989) Binding of pirofen to human serum albumin studied by dialysis and spectroscopy techniques. *Biochem Pharmacol* 38(1):1–7
- Flower DR (1996) The lipocalin protein family: structure and function. *Biochem J* 318(Pt 1):1–14
- Redl B, Holzfeind P, Lottspeich F (1992) cDNA cloning and sequencing reveals human tear prealbumin to be a member of the lipophilic-ligand carrier protein superfamily. *J Biol Chem* 267(28):20282–20287
- Glasgow BJ, Abduragimov AR, Farahbakhsh ZT, Faull KF, Hubbell WL (1995) Tear lipocalins bind a broad array of lipid ligands. *Curr Eye Res* 14(5):363–372
- Gasymov OK, Abduragimov AR, Yusifov TN, Glasgow BJ (1999) Binding studies of tear lipocalin: the role of the conserved tryptophan in maintaining structure, stability and ligand affinity. *Biochim Biophys Acta* 1433(1–2):307–320
- Gasymov OK, Abduragimov AR, Gasimov EO, Yusifov TN, Dooley AN, Glasgow BJ (2004) Tear lipocalin: potential for selective delivery of rifampin. *Biochim Biophys Acta* 1688(2):102–111
- Gasymov OK, Abduragimov AR, Glasgow BJ (2008) Ligand binding site of tear lipocalin: contribution of a trigonal cluster of charged residues probed by 8-anilino-1-naphthalenesulfonic acid. *Biochemistry* 47(5):1414–1424. doi:10.1021/bi701955e
- Breustedt DA, Schonfeld DL, Skerra A (2006) Comparative ligand-binding analysis of ten human lipocalins. *Biochim Biophys Acta* 1764(2):161–173
- Gasymov OK, Abduragimov AR, Glasgow BJ (2007) Characterization of Fluorescence of ANS-TL Complex: Evidence for Multiple Species. *Photochem Photobiol* 83:1405–1414
- Gasymov OK, Abduragimov AR, Glasgow BJ (2009) Intracavitary ligand distribution in tear lipocalin by site-directed tryptophan fluorescence. *Biochemistry* 48(30):7219–7228. doi:10.1021/bi9005557

27. Gasymov OK, Abduragimov AR, Yusifov TN, Glasgow BJ (2000) Resolution of ligand positions by site-directed tryptophan fluorescence in tear lipocalin. *Protein Sci* 9(2):325–331
28. Glasgow BJ, Heinzmann C, Kojis T, Sparkes RS, Mohandas T, Bateman JB (1993) Assignment of tear lipocalin gene to human chromosome 9q34–9qter. *Curr Eye Res* 12(11):1019–1023
29. Glasgow BJ (1995) Tissue expression of lipocalins in human lacrimal and von Ebner's glands: colocalization with lysozyme. *Graefes Arch Clin Exp Ophthalmol* 233(8):513–522
30. Marston FAO (1987) The purification of eukaryotic polypeptides expressed in *Escherichia coli*. In: Glover DM (ed) *DNA Cloning: a practical approach*, vol III, Chap. 4. IRL Press, Oxford, pp 59–88
31. Gasymov OK, Abduragimov AR, Glasgow BJ (2011) The conserved disulfide bond of human tear lipocalin modulates conformation and lipid binding in a ligand selective manner. *Biochim Biophys Acta* 1814(5):671–683. doi:10.1016/j.bbapap.2011.03.017
32. Gasymov OK, Abduragimov AR, Yusifov TN, Glasgow BJ (2003) Resolving near-ultraviolet circular dichroism spectra of single trp mutants in tear lipocalin. *Anal Biochem* 318(2):300–308
33. Lakowicz JR (2006) *Principles of fluorescence spectroscopy*, 3rd edn. Springer, New York
34. Gasymov OK, Abduragimov AR, Yusifov TN, Glasgow BJ (2004) Interstrand loops CD and EF act as pH-dependent gates to regulate fatty acid ligand binding in tear lipocalin. *Biochemistry* 43(40):12894–12904
35. Zimmerman AW, van Moerkerk HT, Veerkamp JH (2001) Ligand specificity and conformational stability of human fatty acid-binding proteins. *Int J Biochem Cell Biol* 33(9):865–876
36. Smithers N, Bolivar JH, Lee AG, East JM (2012) Characterizing the fatty acid binding site in the cavity of potassium channel KcsA. *Biochemistry* 51(40):7996–8002. doi:10.1021/bi3009196
37. Rahman M, Lee EG, Kim SH, Bae YA, Wang H, Yang Y, Kong Y (2012) Characterization of hydrophobic-ligand-binding proteins of *Taenia solium* that are expressed specifically in the adult stage. *Parasitology* 139(10):1361–1374. doi:10.1017/S0031182012000613
38. Drin G, Douguet D, Scarlata S (2006) The pleckstrin homology domain of phospholipase C $\beta$  transmits enzymatic activation through modulation of the membrane-domain orientation. *Biochemistry* 45(18):5712–5724. doi:10.1021/bi052317n
39. Min J, Lee JW, Ahn YH, Chang YT (2007) Combinatorial dapoxy dye library and its application to site selective probe for human serum albumin. *J Comb Chem* 9(6):1079–1083. doi:10.1021/cc0700546
40. Thumser AE, Voysey JE, Wilton DC (1994) The binding of lysophospholipids to rat liver fatty acid-binding protein and albumin. *Biochem J* 301(Pt 3):801–806
41. Martin MP, Alam R, Betzi S, Ingles DJ, Zhu JY, Schonbrunn E (2012) A novel approach to the discovery of small-molecule ligands of CDK2. *Chembiochem* 13(14):2128–2136. doi:10.1002/cbic.201200316
42. Toptygin D, Brand L (1995) Analysis of equilibrium binding data obtained by linear-response spectroscopic techniques. *Anal Biochem* 224(1):330–338. doi:10.1006/abio.1995.1048
43. Toptygin D, Packard BZ, Brand L (1997) Resolution of absorption spectra of rhodamine 6G aggregates in aqueous solution using the law of mass action. *Chem Phys Lett* 277:430–435
44. Jaumot J, Vives M, Gargallo R (2004) Application of multivariate resolution methods to the study of biochemical and biophysical processes. *Anal Biochem* 327(1):1–13. doi:10.1016/j.ab.2003.12.028